Interaction of Charge Density Waves with Defects in Rare-Earth Tritellurides

Saif Siddique, James L Hart, Drake Niedzielski, Ratnadwip Singha, Myung-Geun Han, Noah Schnitzer, Michael Colletta, Mehrdad T Kiani, Stephen D Funni, Natalie Williams, Lena F Kourkoutis, Yimei Zhu, Leslie M Schoop, Tomás A Arias, Judy J Cha



Interaction of Charge Density Waves with Defects in Rare-Earth Tritellurides

Saif Siddigue¹, James L Hart¹, Drake Niedzielski², Ratnadwip Singha³, Myung-Geun Han⁴, Noah Schnitzer¹, Michael Colletta⁵, Mehrdad T Kiani¹, Stephen D Funni¹, Natalie Williams⁶, Lena F Kourkoutis⁵, Yimei Zhu⁴, Leslie M Schoop³, Tomás A Arias², and Judy J Cha^{1,*}

A charge density wave (CDW) is an electronic order in materials with strong electron-phonon interactions and with a periodic modulation in the electron density as well as in the atomic lattice [1]. CDW phases respond strongly to external perturbations such as pressure, strain, disorder, electric and magnetic fields, etc., all of which may suppress the CDW and stabilize competing electronic phases including superconductivity or magnetism [2-4]. Despite the strong electron-lattice coupling in CDW, our understanding of interactions between CDW and structural defects is sparse. Studying the defect-CDW correlation requires both real-space probe to characterize the defects locally and reciprocal-space probe to observe the effects of defects on the CDW. Here, using *in-situ* cryogenic scanning transmission electron microscopy (STEM) and four-dimensional (4D) STEM, we examine the effects of microstructure on the CDW phases of rare-earth tritellurides.

Rare-earth tritellurides (RTe₃; R = rare-earth elements) are layered compounds with square-net Te sheets that give RTe₃ a unique quantum geometry. Recently, an unconventional CDW has been observed in RTe₃[5]. The crystal structure of RTe₃ is weakly orthorhombic, having almost equal in-plane lattice parameters ($|c| - |a| \approx 0.2$ pm, b-axis being the long axis), with the small anisotropy stemming from the presence of a glide plane perpendicular to b and with glide direction only along c(Fig. 1A) [6]. This anisotropy acts as a symmetry breaking field for the CDW phase transition as CDW forms along the c-axis below the transition temperature. For RTe₃ with heavier rare-earth elements (Tb-Tm), a second modulation along a-axis emerges at a lower temperature, creating a bidirectional CDW state [6]. In this work, we show that defect-CDW interactions in RTe₃ reduce the anisotropy between a- and c-axes and as a result change the CDW behavior.

To study the structure and the CDW behavior in RTe₃, we image exfoliated flakes of LaTe₃ and ErTe₃ in both cross-section and plan view. For cross-section samples, we use scotch tape to exfoliate single crystals of LaTe₃ and ErTe₃ on SiO₂/Si substrates to get thin flakes. We then use a focused-ion beam to make cross-section TEM samples in the [100] and [001] zone axes. For plan-view samples, we transfer the exfoliated flakes from SiO₂/Si substrates onto SiN_x TEM grids using polypropylene carbonate (PPC). The samples are imaged at cryogenic temperatures using the Gatan 636 and the HennyZ FDCHB-6 [7] TEM holders in FEI/TFS Titan Themis and TFS Spectra 300 X-CFEG operated at 300 kV. 4D-STEM datasets were collected using the Electron Microscope Pixel Array Detector [8].

Using atomic-resolution STEM imaging on cross-section samples, we observe the presence of basal dislocations in exfoliated flakes of RTe₃ (Fig. 1B). Near the core of dislocation, atomic columns appear smeared due to disorder, and a Burger's circuit analysis reveals a Burger's vector believed to be along [101] direction. Across this dislocation, the layer stacking changes: to the left of the dislocation core, the layer stacking matches that of the [001] projection, and to the right it matches the [100] projection, thus the a- and c-axes are locally swapped. In other words, the direction of the glide switches between the a- and c-axes across the dislocation. If the dislocation density is high, the stacking defect density will be high, as is the case with ErTe₃ (Fig. 1C). Consequently, the glide direction will locally switch between a- and c-axes, converting the system from weakly orthorhombic to pseudo-tetragonal. We expect this to affect the CDW behavior.

To image the CDW response to pseudo-tetragonality due to the presence of dislocations in our ErTe₃ flakes, we acquire selected area electron diffraction (SAED) patterns at ~100 K and quantitatively analyze the CDW superlattice peaks. At this temperature, ErTe₃ should be in a bidirectional CDW state, with ordering wavevectors $q_c = 0.300c^*$ and $q_a = 0.313a^*$ ($|q_a| > |q_c|$) [6]. We use the SAED patterns to compute the average wavevectors in two perpendicular reciprocal lattice directions. First, we get the positions of all Bragg peaks (k_{Bragg}) and CDW superlattice peaks (k_{CDW}) using 2D Gaussian fitting, and then extract the wavevector magnitudes $q = k_{\text{Bragg}} - k_{\text{CDW}}$. For a flake with a low defect density (Fig. 1D), we observe the expected CDW behavior where $|q_2| >$ $|q_1|$. However, a SAED pattern from another flake with a high defect density (Fig. 1E) surprisingly shows $|q_2| \approx |q_1|$, suggesting that when ErTe₃ is in a pseudo-tetragonal state, the high temperature CDW is stabilized in both in-plane directions, and the low temperature CDW is suppressed.

While SAED allowed us to observe this unexpected CDW behavior, it fails to provide a nanoscale picture, particularly the spatial distribution of the CDW near defects. We thus employ 4D-STEM in temperature range 120-300 K with an electron probe size of ~10 nm to understand the local behavior of CDW near extended defects in ErTe₃. Figure 2A shows the virtual dark-field STEM image and diffraction patterns from two real-space pixels of the 4D-STEM data. Going from left to right in the flake, the direction of the most intense CDW peaks changes from the a* axis to the c* axis, suggesting CDW domains. To visualize these domains, we create two sets

¹Department of Materials Science and Engineering, Cornell University, Ithaca, NY, USA

²Department of Physics, Cornell University, Ithaca, NY, USA

³Department of Chemistry, Princeton University, Princeton, NJ, USA

⁴Condensed Matter Physics and Materials Science Department, Brookhaven National Laboratory, Upton, NY, USA

School of Applied and Engineering Physics, Cornell University, Ithaca, NY, USA

⁶Department of Chemistry, Cornell University, Ithaca, NY, USA

^{*}Corresponding author: jc476@cornell.edu

of virtual apertures, which align with the CDW peaks – one for each reciprocal lattice direction (Figs. 2B,C). We then use them to construct real-space maps (Figs. 2D-G show the maps constructed from CDW peaks along a^*). The intensity differences show the spatial variation of the CDW along a^* . At 120 K (Fig. 2D), we find that the ErTe₃ flake has two CDW domains (indicated by a dotted line), where the CDW domain boundaries correlate with dislocation lines observed in the virtual dark field STEM. We also see the temperature evolution of this domain as the temperature is increased, and at T > 200 K, the domain melts away.

We thus demonstrate that defects play an important role in modulating the CDW behaviors in layered RTe₃. Our findings are relevant in developing a microscopic understanding of CDW phase transitions, and possible phase competitions in quantum materials. Additionally, we highlight the promise of *in-situ* cryo-TEM to study the phase transitions in these materials [9].

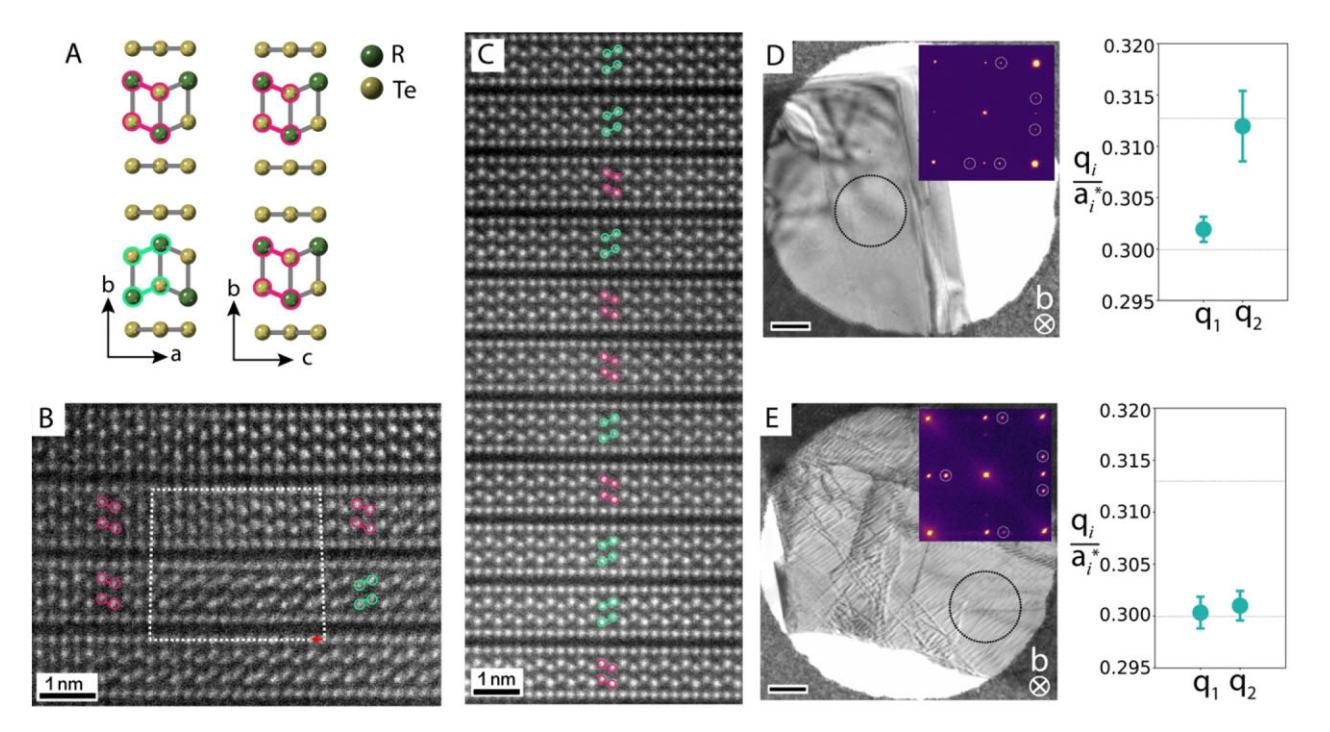


Fig. 1. A. Schematic of crystal structure of RTe₃ when viewed in cross-section. Notice the presence of a c-glide in the [100] zone axis (bc-plane projection). **B.** HAADF-STEM image showing a dislocation core from exfoliated flake of LaTe₃. Projection of Burger's vector in this zone axis is shown in red arrow. The true Burger's vector is along the [101] direction. The stacking order changes across the dislocation core swapping the in-plane axes, and hence the glide direction. **C.** HAADF-STEM image of ErTe₃ in cross-section revealing a high density of stacking defects. Bright-field TEM images of ErTe₃ flakes with (**D**) low defect density and (**E**) high defect density. SAED from the encircled region (inset) of (**D**) shows the expected bulk behavior in terms of wavevector magnitude of CDWs, but for the flake in (**E**) low temperature CDW is suppressed, and high temperature CDW takes its place. Scale bars of (**D**) and (**E**) are 0.25 μm.

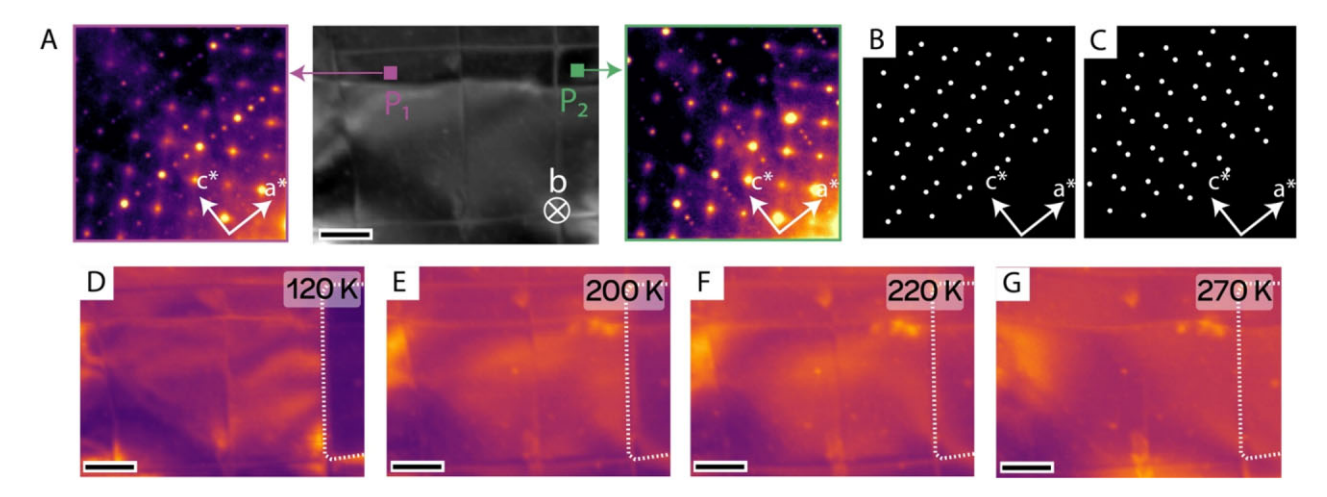


Fig. 2. A. Virtual dark-field STEM image of $ErTe_3$ reconstructed from the 4D-STEM data collected at 120 K. Diffraction patterns from two different pixel positions (P1 and P2) are shown on either side of the virtual image. **B.** and **C.** show the virtual apertures used for selecting the reflections from CDW along each reciprocal lattice direction. **D.**, **E.**, **F.**, and **G** show the real-space maps constructed by applying the virtual aperture || a* at temperatures 120 K, 200 K, 220 K, and 270 K. Scale bars are 0.25 μm.

References

- 1. G Grüner, Rev. Mod. Phys. 60 (1988), p. 1129.
- 2. Gao, et al., Proc. Natl. Acad. Sci. 115 (2018), p. 6986.
- 3. H Weitering et al., Science 285 (1999), p. 2107.
- 4. Y Zhang et al., Phys. Rev. B 66 (2002), p. 094501.
- 5. Y Wang et al., Nature 606 (2022), p. 896.
- 6. N Ru et al., Phys. Rev. B 77 (2008), p. 035114.
- 7. B Goodge et al., Microscopy and Microanalysis 26 (2020), p. 439.
- 8. MW Tate et al., Microscopy and Microanalysis 27 (2016), p. 237.
- 9. The authors acknowledge funding from the DOE, Basic Energy Sciences program (grant DE-SC0023905). This work made use of shared facilities at Cornell supported by NSF: CCMR (DMR-1719875), PARADIM (DMR-2039380) and CNF (NNCI-2025233).





TESCAN FIB-SEM

Drive your materials development and get comprehensive answers.

Fast and effortless!

info.tescan.com/matsci-fib-sem

